Simple Length Determination of Single-Walled Carbon Nanotubes by Viscosity Measurements in Dilute Suspensions

A. Nicholas G. Parra-Vasquez,[†,⊥] Ingrid Stepanek,[†,⊥] Virginia A. Davis,[†,⊥,#] Valerie C. Moore,[‡,⊥] Erik H. Haroz,[§,⊥] Jonah Shaver,[||,⊥] Robert H. Hauge,[‡,⊥] Richard E. Smalley,[‡,⊥,+] and Matteo Pasquali*[,†,‡,⊥]

Department of Chemical and Biomolecular Engineering, MS-362, Department of Chemistry, MS-80, Department of Electrical and Computer Engineering, MS-366, Department of Applied Physics, MS-104, and Carbon Nanotechnology Laboratory, The Richard E. Smalley Institute for Nanoscale Science and Technology, Rice University, 6100 Main St., Houston, Texas 77005

Received August 30, 2006; Revised Manuscript Received March 7, 2007

ABSTRACT: We describe a fast, reproducible method to accurately measure the length of single-walled carbon nanotubes (SWNTs). The method is based on measuring the viscosity of a macroscopic sample of dilute suspended SWNTs. The average length is determined from the difference between the zero-shear viscosity of the suspension and that of the solvent. Using the relationship between viscosity and length, the average length of HiPco SWNTs is found to range from 400 to 700 nm, in agreement with atomic force microscopy (AFM) measurements. Compared to AFM, length determination by viscosity is faster and appears more reproducible.

Introduction

Single-walled carbon nanotubes (SWNTs) have unique mechanical, thermal, and electrical properties;[1] if retained on a macroscopic level, these could be exploited in industrial, biological, and scientific applications, e.g., reinforcing composite materials,[2,3] nanoscopic tunable field effect transistors[4] (semiconducting SWNTs), and nanoscale quantum wires for electronic devices[5,6] as well as macroscopic cables of metallic SWNTs for long-distance power transmission.[7] For these and various other applications, the length of the SWNTs is an important variable.

One example of the importance of length can be shown in fiber spinning. Many techniques have been used to produce fibers containing SWNTs, from composite[8−10] to neat fibers.[11−15] Length of nanotubes is an important variable for solution fiber spinning of neat SWNT fibers in terms of processability of the liquid dispersion as well as the final mechanical, thermal, and electrical properties of the solid fiber. Phase transitions and flow properties of rigid-rod dispersions are affected by length, and SWNTs are no exception.[16−21] SWNT length is believed to play a role in other applications such as the formation of sheets and coatings[22−26] and may affect the interaction of SWNTs with living organisms.[27−30]

Techniques to obtain the molecular weight (or length) of polymers include dynamic[31] and static light scattering,[31] ultracentrifugation,[32] gel permeation chromatography or size exclusion chromatography,[33] matrix-assisted laser desorption/ionization,[34,35] membrane and vapor pressure osmometry,[36] and intrinsic viscosity measurements[37−39] by capillary viscometers. Until recently, none of these methods have been applied successfully to determine the average length of individual SWNTs. The average length and diameter of bundles of SWNTs have been measured by a dynamic light scattering technique.[40] This technique shows great promise; however, it is complicated by the need of making assumptions on effect of light absorption by SWNTs. The length distribution of a suspension of SWNTs was measured by dynamic light scattering in combination with zeta potential measurements.[41] In this case, however, the model used to interpret the measurements assumes that the SWNT length is much smaller than the wavelength of light.

The most common method of obtaining both average length and length distribution of SWNTs has been atomic force microscopy (AFM). This technique, however, is time-consuming, is preparation sensitive, has small sample sizes (200−2000 SWNTs), and relies on subjective height thresholding (human or computer-aided) to identify SWNTs[42−45]—of course, sample preparation and image analysis are faster if individual SWNTs and bundles are not differentiated. A faster, preparation-insensitive, objective method for measuring SWNT length is preferable.

This paper describes a quick method for measuring the average length of SWNT sample through viscosity measurements on a dilute dispersion of individual SWNTs.

Theory

The zero-shear viscosity η_0 is the limiting value of the ratio of measured shear stress σ to imposed shear rate κ as the shear rate tends to zero. In a solution or suspension, η_0 is the sum of the solvent viscosity η_s and a contribution due to the suspended objects. When such solution or suspension is dilute, molecules or particles do not interact with each other; therefore, the change in viscosity of such dilute fluids depends linearly on the concentration of the suspended objects.

In a dilute suspension of rods, the zero-shear viscosity can be expressed as[46,47]

$$\eta_0 = \frac{\sigma}{\kappa} = \eta_s + \frac{2}{15}\nu\varsigma_r \tag{1}$$

* Corresponding author. E-mail: mp@rice.edu.
† Department of Chemical and Biomolecular Engineering.
‡ Department of Chemistry.
§ Department of Electrical and Computer Engineering.
|| Department of Applied Physics.
⊥ The Richard E. Smalley Institute for Nanoscale Science and Technology.
Current address: Department of Chemical Engineering, 230 Ross Hall, Auburn University, Auburn, AL 36849-5127.
+ Deceased: October 28, 2005.

10.1021/ma062003n CCC: $37.00
Published on Web 04/28/2007

For monodisperse rods, the number of rods per unit volume ν is the ratio of the volume fraction ϕ of rods in solution to the volume of one rod

$$\nu \equiv \frac{\phi}{\pi R^2 L} \tag{2}$$

where R and L denote the rod radius and length, respectively. In a SWNT, R should be identified with the distance between the SWNT axis and a carbon atom plus the van der Waals radius of a carbon atom. The rotational friction coefficient ς_r can be related to the dimensions of the rod by assuming that the rod is slender, the flow is laminar, and the fluid sticks to the surface of the rod. Under these assumptions[48,49]

$$\varsigma_r = \frac{\pi \eta_s L_s^3}{3} \epsilon f(\epsilon) \tag{3}$$

where

$$\epsilon = \frac{1}{\ln\left(\frac{L_s}{R_s}\right)} \tag{4}$$

and

$$f(\epsilon) = \frac{1 + 0.64\epsilon}{1 - 1.5\epsilon} + 1.659\epsilon^2 \tag{5}$$

where L_s and R_s refer to the axial and radial locations where the fluid adheres to the rod. In a SWNT−surfactant complex, $L \approx L_s$ because any surfactant adsorbed at the SWNT ends (few nanometers length) does not affect considerably the overall length of the SWNT−surfactant complex (hundreds of nanometers). Conversely, the effect of the surfactant size a must be considered in estimating the effective radius of the SWNT−surfactant complex as $R_s = R + a$.

Rearranging (1) and combining (2) and (3) gives the intrinsic viscosity $[\eta]$ of a dilute Brownian dispersion of rods (monodisperse in length L and diameter D, with the aspect ratio $A = L/D$):

$$[\eta] \equiv \lim_{\phi \to 0} \frac{\eta_0 - \eta_s}{\eta_s \phi} = \frac{8}{45}\left(\frac{L}{D}\right)^2 \epsilon f(\epsilon) \tag{6}$$

The effect of the surfactant on the radius R_s is in the correction factor ϵ. Equation 6 shows that the length of rods of known diameter in a suspension can be determined from a zero-shear viscosity measurement.

SWNT samples are polydisperse in both length and diameter; therefore, eq 6 should be extended to polydisperse systems. There is no information on whether SWNT diameter and length are correlated; hereafter, they are assumed to be uncorrelated. The diameter distribution of HiPco SWNTs is so narrow ($D = 0.98 \pm 0.21$ nm for an estimate[50]) that treating the sample as monodisperse in diameter introduces minimal approximation (e.g., $\langle D \rangle^2$ and $\langle D^2 \rangle$ differ by about 5%); therefore, the SWNTs are considered monodisperse in diameter hereafter. Equation 6 holds for a sample of rods monodisperse in diameter and polydisperse in length if the length L is replaced by defining a "viscosity average length'':

$$L_{visc} \equiv \sqrt{\frac{\langle L^3 \rangle}{\langle L \rangle}} \tag{7}$$

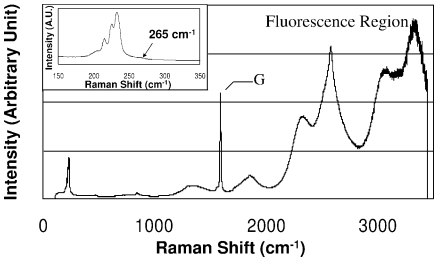

Figure 1. A fluorescence signal (seen at Raman shifts greater than 2000 cm^{-1}) stronger than the G peak (1593 cm^{-1}) and the absence of the roping peak (265−267 cm^{-1}) show that the dispersion consists almost exclusively of individual SWNTs. The excitation wavelength used was 785 nm.

where $\langle L \rangle$ and $\langle L^3 \rangle$ are the first and third moments of the length distribution, respectively, defined for a finite population of rods as

$$\langle L^n \rangle = \frac{\sum_{i=1}^{N} L_i^n}{N} \tag{8}$$

where N is the total number of rods and n is the moment of interest. Therefore, in a polydisperse sample the intrinsic viscosity measures the ratio of the third and first moments of the length distribution.

Experimental Procedures

Surfactant-stabilized SWNT dispersions (from HiPco produced SWNTs at Rice University, HPR 120.3) were prepared by sonication and centrifugation followed by decanting.[51,52] By combining the average carbon−carbon diameter of HiPco material, 0.93 nm,[53] to twice the van der Waals radius of carbon, 0.17 nm, we estimate that the average external diameter of the SWNTs in our sample is $D = 1.27$ nm.

The two surfactants used were pluronics F-68 (BASF): a poly(ethylene oxide)−poly(propylene oxide)−poly(ethylene oxide) (PEO_{80}−PPO_{30}−PEO_{80}) triblock surfactant with an average molecular weight of 8400 g/mol and sodium dodecyl sulfate (SDS, from Sigma Aldrich), a small surfactant with a molecular weight of 288 g/mol. A 2 wt % solution of pluronic F-68 and a 1 wt % solution of SDS in water were used to suspend SWNTs. This is the ideal range suggested by Wang et al. to minimize potential depletion effects.[54] The size of the PEO chain protruding from the surface is highly dependent on the curvature of the surface;[55] because of the high curvature of SWNTs, the protrusion can be estimated by its Flory radius of $lN^{3/5} = (0.24\text{ nm})(76)^{3/5} \approx 3.2$ nm, where l is the size of a monomer and N is the number of monomers. The size of SDS micelles[56] is similar to the size of SDS protruding from the surface of SWNTs,[57] giving a protrusion of 2.25 ± 0.25 nm.

The concentrations of the solutions were measured by UV−vis spectroscopy using the extinction coefficient 0.043 L/(mg cm) at 763 nm.[58] The concentrations were converted to volume fraction, which was used to calculate number density, by using a SWNT tube density of 1.45 g/cm^3 (close-packed density for (7,8) SWNTs). Low concentrations were tested to ensure that measurements were in the dilute regime; this occurs for dispersions with viscosities roughly below twice the solvent viscosity.[47] The dispersion with the highest concentration was diluted to make several different concentrations. Dispersions at low concentrations with viscosities within 5% of the solvent were not used because of the large subtraction error when calculating the reduced viscosity, $\eta_{red} \equiv (\eta - \eta_s)/\eta_s\phi$. Raman spectroscopy was done using 785 nm excitation wavelength and 1.5 mW beam power (on Holoprobe Research Raman microscope, Kaiser Optical Systems Inc.). Raman on the most concentrated dispersion (Figure 1) showed that the dispersions

contained at least 90% individuals, evidenced by a strong fluorescence peak (greater than the G peak, 1593 cm^{-1})[51] and the absence of the roping peak (265−267 cm^{-1}).[59]

Each diluted sample was tested (on an ARES strain-controlled rheometer, Rheometrics Scientific, now TA Instruments) at shear rates $\dot{\gamma}$ from 1 to 100 s^{-1} in a Couette fixture (height 34 mm, cup diameter 34 mm, bob diameter 32 mm, 1 mm gap, torque sensitivity $\sim 0.1\ \mu$N·m, corresponding to a minimum measurable shear stress of 1.83 mPa). A vapor trap was used to maintain a moisture-saturated environment preventing solvent evaporation.

AFM (NanoScope R IIIa, Veeco Instruments) samples were prepared by dip-coating the dispersions on aminated silicon wafers. The amination process began with a series consisting of a hydrofluoric acid cleaning step (15 min) and an ozonation step (30 min) to oxidize the surface for better functionalization. The silicon wafer was then soaked in a solution of 4−6 drops of 3-aminopropyltriethoxysilane in 15 mL of chloroform for 15 min and rinsed; during the whole process the top surface of the silicon wafer remained face-up to prevent contamination. The SWNTs were deposited onto the wafer by dip-coating and then rinsed with isopropanol and dried with pure nitrogen for imaging.

Results and Discussion

The aspect ratio of SWNTs was determined by measuring the zero-shear viscosity of dilute suspensions of individual SWNTs stabilized in water with surfactants. Length distributions were also measured by AFM to estimate the relative merit of the two measurements.

Viscosity. In the first study, a pluronic F-68 dispersion at a concentration of 51 ppm vol (74 mg/L) was diluted to two lower concentrations, as low as 19 ppm vol (28 mg/L). Figure 2a shows the specific viscosity, $\eta_{sp} \equiv (\eta - \eta_s)/\eta_s$, of these dispersions increases with concentration and shear thins at higher shear rates.

In the dilute regime, the viscosity is expected to increase linearly with concentration. The rotational relaxation time τ_{rot} should not depend on concentration because the SWNTs in a dilute solution are not interacting; in rods, τ_{rot} scales roughly with the third power of the rod length,[47] as confirmed recently by measurements on individual SWNTs,[60] as defined below:

$$\tau_{rot} \equiv \frac{\pi \eta_s L^3}{18 k_B T} \epsilon f(\epsilon) \qquad (9)$$

Therefore, the reduced viscosity η_{red} of dilute suspensions should overlay at all shear rates. Figure 2b shows that this is indeed the case for suspensions of pluronic-stabilized SWNTs below 51 ppm vol. Importantly, Figure 2b shows that all the suspensions transition at the same shear rate (roughly 10 s^{-1}) from a regime where the viscosity is independent of shear rate to a regime where the viscosity decreases with shear rate. Theory dictates that the transition should occur when $\dot{\gamma}\tau_{rot} \geq 1$, i.e., when the hydrodynamic drag torque on the rods exceeds the Brownian torque due to the fluctuating momentum exchange between the rod and the liquid. Therefore, the various samples are dilute, and the SWNTs in the samples are not bundled—otherwise, this would alter the length distribution, which in turn would alter the shear rate where this transition occurs. The intrinsic viscosity is extracted from the data in Figure 2 by averaging all the viscosity measurements below $\dot{\gamma} \approx 10\ s^{-1}$. This yields $[\eta] = 7735 \pm 500$, corresponding to a viscosity average length $L_{visc} = 500 \pm 40$ nm.

In a second study, SDS was used to stabilize the SWNTs. The most concentrated dispersion, 25 ppm vol (36 mg/L), was diluted to three different concentrations, as low as 13 ppm vol (19 mg/L). As shown in Figure 2c, the reduced viscosities overlay at all shear rates, resulting in an intrinsic viscosity of 7350 ± 550, corresponding to a viscosity average length of 505 ± 35 nm.

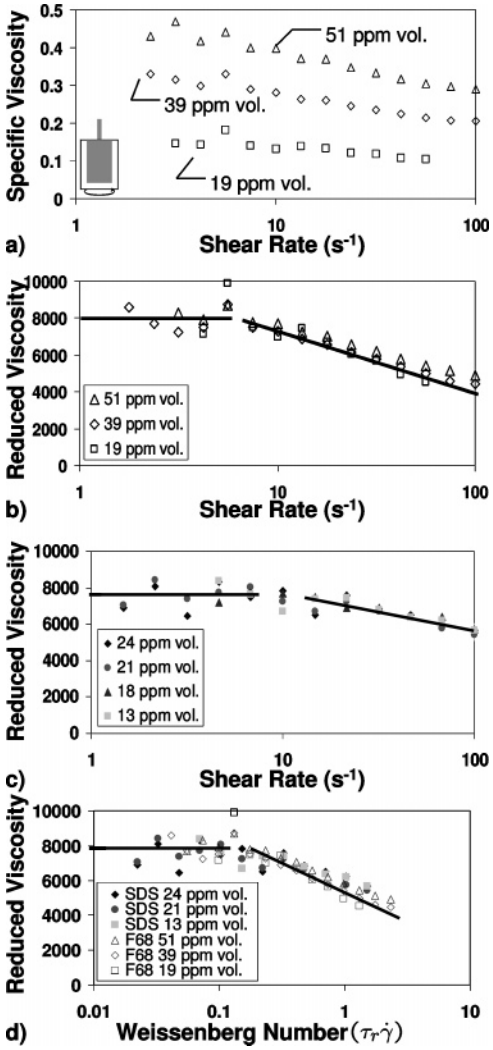

Figure 2. (a) Specific viscosity, $\eta_{sp} \equiv (\eta - \eta_s)/\eta_s$, of SWNTs dispersed in Pluronic F68 show that the viscosity increases with concentration and begins to shear thin at high shear rates. (b) Reduced viscosity, $\eta_{red} \equiv \eta_{sp}/\phi$, of SWNTs dispersed in Pluronic F68 overlay at all shear rates and plateau to the zero-shear reduced viscosity, giving a viscosity average aspect ratio of 500 ± 40. (c) Reduced viscosity of SWNTs dispersed in SDS overlay at all shear rates and plateau to the zero-shear reduced viscosity, giving a viscosity average aspect ratio of 505 ± 35. (d) Reduced viscosity for both surfactants overlay at all Weissenberg numbers as predicted by the theory of dilute suspensions of Brownian rods.

Rigid-rod theory predicts that the reduced viscosity of dilute suspensions should only be a function of the rod's radius and average length. Because the experiments described above were performed with the same HiPco batch of SWNTs, the rods remained the same; therefore, the reduced viscosity should be independent of concentration and surfactant used. Figure 2d shows that the reduced viscosities of both the pluronics and SDS dispersions overlay with excellent agreement, within experimental error, at all Weissenberg numbers, $Wi \equiv \tau_{rot}\dot{\gamma}$, yielding the viscosity average lengths of 500 and 505 nm for pluronic and SDS dispersions, respectively. The Weissenberg number is a dimensionless number scaling the shear rates $\dot{\gamma}$ by the rotational relaxation time τ_{rot} calculated for $L = L_{visc}$—equivalently, the rotary Peclet number can be used, $Pe_r \equiv (\dot{\gamma}/D_{rot})$, where D_{rot} is the rotational diffusion coefficient,[47] $D_{rot} \equiv$

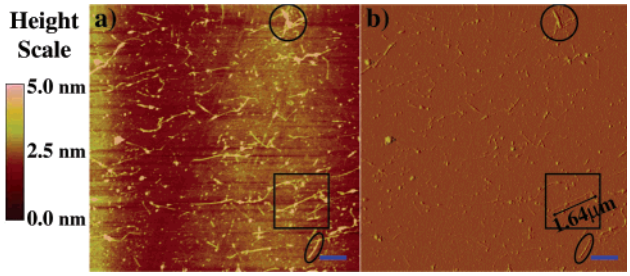

Figure 3. AFM image of mostly individual (boxed) and some bundled (circled) SWNTs. The left image shows the height data, brighter means higher (up to 5 nm), and the right image shows the amplitude data. SWNT lengths can easily reach 1.5 μm. The scale bar is 1 μm.

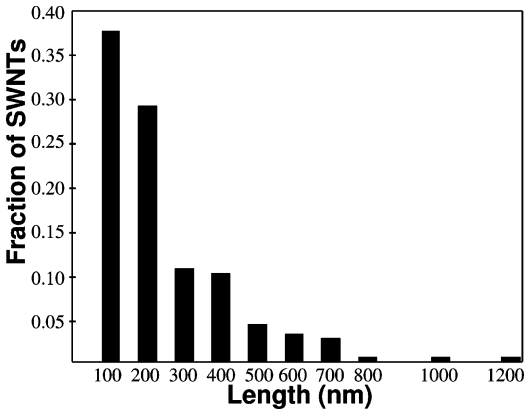

Figure 4. Histogram of lengths obtained through AFM yielding a viscosity average length of 457 nm.

$1/(6\tau_{rot})$. The experimental data at lower shear rates are noisy due to the sensitivity limit of the torque transducer.

AFM. Up to now, SWNT length has been measured mostly by atomic force microscopy (AFM). However, in order to produce reliable images with AFM, individual SWNTs must be deposited, dried, and washed onto an ultraflat surface; all can induce artifacts. The length scales of importance are in the 1−3 nm range, where the height is used to distinguish individuals from bundles. The AFM samples were prepared from the same pluronic-stabilized dispersions.

Figure 3 shows that most of the nanotubes deposited are individuals; the height image (Figure 3a) was used to ensure that individuals and not bundles of SWNTs were measured. Translating AFM images into length distributions requires choosing a cutoff height that distinguishes between individual SWNTs and bundles (presumably formed during the drying of the sample). The height cutoff is not well-defined because SWNTs are coated by surfactant, and the height of the dried surfactant layer is unknown. For example, an image with height of 5 nm could represent one SWNT with a thick pluronic coating, or two SWNTs with less surfactant (see, e.g., the oval in Figure 3). Here, images with a height between 1 and 3 nm were taken to represent individuals; sampling heights along the tube as well as computer-aided software (Nanotube Length Analysis package of SIMAGIS software, Smart Imaging Technologies, Houston, TX) were used to determine individual SWNTs. For the pluronic-stabilized dispersion, ten 10 × 10 μm^2 areas on an AFM sample were imaged to accumulate lengths of 188 individual SWNTs ranging from 50 to 1180 nm. The distribution of length is shown in Figure 4.

The viscosity method measures the viscosity average length defined in eq 7; to compare viscosity and AFM, the same average length must be calculated from the AFM length distribution. The viscosity average length determined from the AFM distribution is 457 nm, 10% below the value measured by viscosity (500 nm).

Table 1. Viscosity Average Lengths (L_{visc}, nm) Measured by Viscosity and AFM

	sample 1	sample 2
viscosity	500 ± 40	680 ± 80
AFM	457 ± 45	953 ± 50

AFM vs Viscosity. To check reproducibility, a second pluronic-stabilized sample was prepared by sonication and ultracentrifugation from the same HiPco batch. Length was measured by both viscosity and AFM (792 SWNTs), yielding average lengths of 680 and 953 nm, respectively (33% difference). Table 1 summarizes the values of L_{visc} measured by viscosity and AFM on two samples. The two viscosity measurements differ by about 30%, while the two AFM measurements are off by more than a factor of 2.

Instrument sensitivity can only account for 5−10% of the difference in viscosity measurements. The remaining 20−25% must be due to dispersion preparation (e.g., sonication can shorten SWNTs). The AFM measurements will have this same 20−25% difference due to dispersion preparation; the remaining difference is due to the poor reproducibility of AFM sample preparation and analysis. Typically, AFM sample preparation results in differences as high as 30% arising from the number of dips, the difference in sample sizes, and the differences in the wafer surfaces. To assess subjectivity of AFM analysis, two of us (A.N.G.P.V. and E.H.H.) independently analyzed the same AFM images using the same acceptance criterion (1−3 nm in height) and reported results that differed by 13%. As a second test, one long tube of length 1640 nm was artificially added to the sample with the viscosity average length of 457 nm; its viscosity average length increased by 16%. The preparation of a surfactant-stabilized suspension of individual SWNTs typically takes 5 h. The viscosity method requires 2−3 h; AFM requires about 8−10 h to deposit SWNTs on surfaces and acquire sufficient images (200−2000 SWNTs) and about 8 h to analyze the data by computer software. In AFM, a small number of tubes (200−2000) are imaged and viewed as representative of the bulk sample, while in the viscosity measurements roughly 10^{15} tubes are used. Therefore, we believe that viscosity is a more objective, reproducible, and effective way of measuring the average length of SWNTs and as future work will show length distribution.

Conclusion

The zero-shear viscosity of dilute dispersions of SWNTs can be used to quantify the average length of SWNTs. This measurement agrees within 10−30% with the viscosity average length measured by AFM. A repeat test suggests that AFM results have a higher variability than viscosity measurements. The difference is believed to be due to poor reproducibility of AFM analysis because of small sample sizes, sample preparation technique, and image analysis. A better understanding of the relative merits of various techniques (AFM, light scattering, viscosity, etc.) for measuring SWNT length could be achieved by comparing the results of such techniques on well-controlled, standardized samples.

Acknowledgment. We gratefully acknowledge useful discussions with Erik Hobbie, Rajat Duggal, Sean Kohl, Howard Schmidt, Jason Longoria, and Valentin Prieto. This work was funded by the DURINT initiative of the Office of Naval Research under Contract N00014- 01-1-0789, by the NSF Center for Biological and Environmental Nanotechnology (EEC-

0118007) and NSF award (CBET-0508498), and by the Advanced Technology Program of the state of Texas under Grant 003604-0113-2003.

References and Notes

(1) Baughman, R. H.; Zakhidov, A. A.; de Heer, W. A. *Science* **2002**, *297*, 787−792.
(2) Andrews, R.; Jacques, D.; Rao, A. M.; Rantell, T.; Derbyshire, F.; Chen, Y.; Chen, J.; Haddon, R. C. *Appl. Phys. Lett.* **1999**, *75*, 1329−1331.
(3) Bryning, M. B.; Milkie, D. E.; Islam, M. F.; Kikkawa, J. M.; Yodh, A. G. *Appl. Phys. Lett.* **2005**, *87*, 161909.
(4) Appenzeller, J.; Martel, R.; Derycke, V.; Radosavjevic, M.; Wind, S.; Neumayer, D.; Avouris, P. *Microelectron. Eng.* **2002**, *64*, 391−397.
(5) Choi, H. J.; Ihm, J.; Louie, S. G.; Cohen, M. L. *Phys. Rev. Lett.* **2000**, *84*, 2917−2920.
(6) Johnston, D. E.; Islam, M. F.; Yodh, A. G.; Johnson, A. T. *Nat. Mater.* **2005**, *4*, 589−592.
(7) Smalley, R. E. "Testimony to the US House of Representatives Committee on Science, Energy Subcommittee Hearing'', Dec 4, 2003.
(8) Dalton, A. B.; Collins, S.; Munoz, E.; Razal, J. M.; Ebron, V. H.; Ferraris, J. P.; Coleman, J. N.; Kim, B. G.; Baughman, R. H. *Nature (London)* **2003**, *423*, 703−703.
(9) Kumar, S.; Dang, T. D.; Arnold, F. E.; Bhattacharyya, A. R.; Min, B. G.; Zhang, X. F.; Vaia, R. A.; Park, C.; Adams, W. W.; Hauge, R. H.; Smalley, R. E.; Ramesh, S.; Willis, P. A. *Macromolecules* **2002**, *35*, 9039−9043.
(10) Vigolo, B.; Penicaud, A.; Coulon, C.; Sauder, C.; Pailler, R.; Journet, C.; Bernier, P.; Poulin, P. *Science* **2000**, *290*, 1331−1334.
(11) Gommans, H. H.; Alldredge, J. W.; Tashiro, H.; Park, J.; Magnuson, J.; Rinzler, A. G. *J. Appl. Phys.* **2000**, *88*, 2509−2514.
(12) Jiang, K. L.; Li, Q. Q.; Fan, S. S. *Nature (London)* **2002**, *419*, 801−801.
(13) Li, Y. L.; Kinloch, I. A.; Windle, A. H. *Science* **2004**, *304*, 276−278.
(14) Zhu, H. W.; Xu, C. L.; Wu, D. H.; Wei, B. Q.; Vajtai, R.; Ajayan, P. M. *Science* **2002**, *296*, 884−886.
(15) Ericson, L. M.; et al. *Science* **2004**, *305*, 1447−1450.
(16) Davis, V. A.; Ericson, L. M.; Parra-Vasquez, A. N. G.; Fan, H.; Wang, Y. H.; Prieto, V.; Longoria, J. A.; Ramesh, S.; Saini, R. K.; Kittrell, C.; Billups, W. E.; Adams, W. W.; Hauge, R. H.; Smalley, R. E.; Pasquali, M. *Macromolecules* **2004**, *37*, 154−160.
(17) Chen, Z. Y. *Phys. Rev. E: Stat. Phys.* **1994**, *50*, 2849−2855.
(18) Forest, M. G.; Wang, Q. *Rheol. Acta* **2003**, *42*, 20−46.
(19) Fry, D.; Langhorst, B.; Kim, H.; Grulke, E.; Wang, H.; Hobbie, E. K. *Phys. Rev. Lett.* **2005**, *95*, 038304.
(20) Fry, D.; Langhorst, B.; Wang, H.; Becker, M. L.; Bauer, B. J.; Grulke, E. A.; Hobbie, E. K. *J. Chem. Phys.* **2006**, *124*, 054703.
(21) Hemmer, P. C. *Mol. Phys.* **1999**, *96*, 1153−1157.
(22) Duggal, R.; Hussain, F.; Pasquali, M. *Adv. Mater.* **2006**, *18*, 29−34.
(23) Meitl, M. A.; Zhou, Y. X.; Gaur, A.; Jeon, S.; Usrey, M. L.; Strano, M. S.; Rogers, J. A. *Nano Lett.* **2004**, *4*, 1643−1647.
(24) Trottier, C. M.; Glatkowski, P.; Wallis, P.; Luo, J. *J. Soc. Inf. Disp.* **2005**, *13*, 759−763.
(25) Wu, Z. C.; Chen, Z. H.; Du, X.; Logan, J. M.; Sippel, J.; Nikolou, M.; Kamaras, K.; Reynolds, J. R.; Tanner, D. B.; Hebard, A. F.; Rinzler, A. G. *Science* **2004**, *305*, 1273−1276.
(26) Zhang, X. F.; Sreekumar, T. V.; Liu, T.; Kumar, S. *J. Phys. Chem. B* **2004**, *108*, 16435−16440.
(27) Cherukuri, P.; Bachilo, S. M.; Litovsky, S. H.; Weisman, R. B. *J. Am. Chem. Soc.* **2004**, *126*, 15638−15639.
(28) Fiorito, S.; Serafino, A.; Andreola, F.; Bernier, P. *Carbon* **2006**, *44*, 1100−1105.
(29) Nimmagadda, A.; Thurston, K.; Nollert, M. U.; McFetridge, P. S. F. *J. Biomed. Mater. Res., Part A* **2006**, *76A*, 614−625.
(30) Sayes, C. M.; Liang, F.; Hudson, J. L.; Mendez, J.; Guo, W. H.; Beach, J. M.; Moore, V. C.; Doyle, C. D.; West, J. L.; Billups, W. E.; Ausman, K. D.; Colvin, V. L. *Toxicol. Lett.* **2006**, *161*, 135−142.
(31) Muller, A.; Burchard, W. *Colloid Polym. Sci.* **1995**, *273*, 866−875.
(32) Ohoya, S.; Hasegawa, T.; Tsubakiyama, K.; Matsuo, T. *Polym. J.* **2001**, *33*, 113−120.
(33) Styring, M. G., Hamielec, A. E., Cooper, A. R., Eds. *Chemical Analysis*; John Wiley and Sons: New York, 1989; Vol. 103.
(34) Creel, H. *Trends Polym. Sci.* **1993**, *1*, 336−342.
(35) Tatro, S. R.; Baker, G. R.; Fleming, R.; Harmon, J. P. *Polymer* **2002**, *43*, 2329−2335.
(36) Lehmann, U.; Kohler, W.; Albrecht, W. *Macromolecules* **1996**, *29*, 3212−3215.
(37) Fuoss, R. M. *Discuss. Faraday Soc.* **1951**, *11*, 125.
(38) Yamanaka, J.; Matsuoka, H.; Kitano, H.; Ise, N. *J. Colloid Interface Sci.* **1990**, *134*, 92−106.
(39) Yamanaka, J.; Matsuoka, H.; Kitano, H.; Hasegawa, M.; Ise, N. *J. Am. Chem. Soc.* **1990**, *112*, 587−592.
(40) Badaire, S.; Poulin, P.; Maugey, M.; Zakri, C. *Langmuir* **2004**, *20*, 10367−10370.
(41) Lee, J. Y.; Kim, J. S.; An, K. H.; Lee, K.; Kim, D. Y.; Bae, D. J.; Lee, Y. H. *J. Nanosci. Nanotechnol.* **2005**, *5*, 1045−1049.
(42) Islam, M. F.; Rojas, E.; Bergey, D. M.; Johnson, A. T.; Yodh, A. G. *Nano Lett.* **2003**, *3*, 269−273.
(43) Zaric, S.; Ostojic, G. N.; Kono, J.; Shaver, J.; Moore, V. C.; Hauge, R. H.; Smalley, R. E.; Xing, W. *Nano Lett.* **2004**, *4*, 2219−2221.
(44) Wang, S.; Liang, Z.; Wang, B.; Zhang, C. *Nanotechnology* **2006**, *17*, 634−639.
(45) Ziegler, K. J.; Gu, Z. N.; Shaver, J.; Chen, Z. Y.; Flor, E. L.; Schmidt, D. J.; Chan, C.; Hauge, R. H.; Smalley, R. E. *Nanotechnology* **2005**, *16*, S539−S544.
(46) Kirkwood, J. G.; Auer, P. L. *J. Chem. Phys.* **1951**, *19*, 281.
(47) Doi, M.; Edwards, S. F. *The Theory of Polymer Dynamics;* Oxford University Press: New York, 1986.
(48) Batchelor, G. K. *J. Fluid Mech.* **1970**, *41*, 545.
(49) Larson, R. G. *The Structure and Rheology of Complex Fluids;* Oxford University Press: New York, 1999.
(50) Kukovecz, A.; Kramberger, C.; Georgakilas, V.; Prato, M.; Kuzmany, H. *Eur. Phys. J. B* **2002**, *28*, 223−230.
(51) Moore, V. C.; Strano, M. S.; Haroz, E. H.; Hauge, R. H.; Smalley, R. E.; Schmidt, J.; Talmon, Y. *Nano Lett.* **2003**, *3*, 1379−1382.
(52) O'Connell, M. J.; Bachilo, S. M.; Huffman, C. B.; Moore, V. C.; Strano, M. S.; Haroz, E. H.; Rialon, K. L.; Boul, P. J.; Noon, W. H.; Kittrell, C.; Ma, J. P.; Hauge, R. H.; Weisman, R. B.; Smalley, R. E. *Science* **2002**, *297*, 593−596.
(53) Bachilo, S. M.; Strano, M. S.; Kittrell, C.; Hauge, R. H.; Smalley, R. E.; Weisman, R. B. *Science* **2002**, *298*, 2361−2366.
(54) Wang, H.; Zhou, W.; Ho, D. L.; Winey, K. I.; Fischer, J. E.; Glinka, C. J.; Hobbie, E. K. *Nano Lett.* **2004**, *4*, 1789−1793.
(55) Li, J. T.; Caldwell, K. D.; Rapoport, N. *Langmuir* **1994**, *10*, 4475−4482.
(56) Bibette, J.; Roux, D.; Nallet, F. *Phys. Rev. Lett.* **1990**, *65*, 2470−2473.
(57) Richard, C.; Balavoine, F.; Schultz, P.; Ebbesen, T. W.; Mioskowski, C. *Science* **2003**, *300*, 775−778.
(58) Moore, V. C. Single walled carbon nanotubes: Suspension in aqueous/surfactant media and chirality controlled synthesis on surfaces. Ph.D. Thesis, Rice University, 2005.
(59) O'Connell, M. J.; Sivaram, S.; Doorn, S. K. *Phys. Rev. B* **2004**, *69*, 235415.
(60) Duggal, R.; Pasquali, M. *Phys. Rev. Lett.* **2006**, *96*, 246104.

MA062003N